NeuroImage 47 (2009) 1312–1318

Contents lists available at ScienceDirect

NeuroImage

journal homepage: www.elsevier.com/locate/ynimg

Measurement of cerebral blood volume in mouse brain regions using micro-computed tomography

Brige P. Chugh [a,b,*], Jason P. Lerch [a], Lisa X. Yu [a], Martin Pienkowski [c,d], Robert V. Harrison [e], R. Mark Henkelman [a,b], John G. Sled [a,b]

[a] Mouse Imaging Centre, The Hospital for Sick Children, Toronto Centre for Phenogenomics, 25 Orde Street Toronto, Ontario, Canada, M5T 3H7
[b] Department of Medical Biophysics, University of Toronto, Toronto, ON Canada
[c] Department of Physiology and Biophysics, University of Calgary, Calgary, Canada
[d] Department of Psychology, University of Calgary, Calgary, Canada
[e] Department of Otolaryngology-HNS, The Hospital for Sick Children and University of Toronto, Toronto, Ontario, Canada

ARTICLE INFO

Article history:
Received 30 January 2009
Revised 9 March 2009
Accepted 31 March 2009
Available online 9 April 2009

Keywords:
Cerebral blood volume
Mice
micro-CT
Microvasculature

ABSTRACT

Micro-computed tomography (micro-CT) is an X-ray imaging technique that can produce detailed 3D images of cerebral vasculature. This paper describes the development of a novel method for using micro-CT to measure cerebral blood volume (CBV) in the mouse brain. As an application of the methodology, we test the hypotheses that differences in CBV exist over anatomical brain regions and that high energy demanding primary sensory regions of the cortex have locally elevated CBV, which may reflect a vascular specialization. CBV was measured as the percentage of tissue space occupied by a radio-opaque silicon rubber that fills the vasculature. To ensure accuracy of the CBV measurements, several innovative refinements were made to standard micro-CT specimen preparation and analysis procedures. Key features of the described method are vascular perfusion under controlled pressure, registration of the micro-CT images to an MRI anatomical brain atlas and re-scaling of micro-CT intensities to CBV units with selectable exclusion of major vessels. Histological validation of the vascular perfusion showed that the average percentage of vessels filled was $93 \pm 3\%$. Comparison of thirteen brain regions in nine mice revealed significant differences in CBV between regions ($p < 0.0001$) while cortical maps showed that primary visual and auditory areas have higher CBV than primary somatosensory areas.

Introduction

Micro-computed tomography (micro-CT) can provide detailed 3D images of the mouse vascular architecture (Ritman, 2004). Recent applications of micro-CT to the mouse cerebral circulation include the systematic classification of major vessels (Dorr et al., 2007), the detection of atherosclerotic lesions around the circle of Willis (Langheinrich et al., 2007), and the co-registration of capillary-level views of the circulation with the macroscopic vasculature (Heinzer et al., 2006). The use of this technique in the mouse is motivated by a desire to better understand mouse models of human diseases.

This paper describes the application of micro-CT to measure cerebral blood volume (CBV) for characterizing total vascularity in 3D regions of the mouse brain. CBV is defined as the total volume of blood in a given unit volume of brain (Toga and Mazziotta, 2002). Measurement of CBV in local regions of the mouse brain is of particular interest for delineating the phenotypes of models of neurodegenerative diseases that alter cerebral vasculature, such as Alzheimer's disease (Buee et al., 1997).

Before the advent of suitable 3D imaging technologies, the CBV of the whole mouse brain was measured by detecting intravascular radionuclides (Edvinsson et al., 1973). More recently, regional values of CBV were obtained using magnetic resonance imaging (MRI) (Wu et al., 2003); however, resolution was limited to $0.1\ \text{mm} \times 0.1\ \text{mm} \times 0.6\ \text{mm}$ due to the time constraints of in vivo MRI scanning. Another technique that allows a higher resolution for CBV mapping is multi-photon laser scanning microscopy (Verant et al., 2007); however, available optics and depth of light penetration limit this technique to the superficial 0.6 mm of cortex over small fields of view. Micro-CT measurement of CBV provides both high-resolution and whole brain coverage for characterizing 3D regions.

In this paper, we present a methodology by which CBV can be measured as the percentage of a volume of tissue occupied by a perfused radio-opaque silicon rubber that remains intravascular. We utilize the principle that for a voxel filled with two components, tissue and radio-opaque contrast agent, the micro-CT image intensity is a weighted average of the attenuation coefficients of each component

* Corresponding author. Mouse Imaging Centre, Hospital for Sick Children, Toronto Centre for Phenogenomics, 25 Orde Street, Toronto, Ontario, Canada, M5T 3H7. Fax: +1 647 837 5832.
E-mail address: brige@phenogenomics.ca (B.P. Chugh).

1053-8119/$ – see front matter © 2009 Elsevier Inc. All rights reserved.
doi:10.1016/j.neuroimage.2009.03.083

(Goodenough et al., 1986). Thus, the micro-CT image intensity is linearly related to the proportion of a voxel's volume that is occupied by radio-opaque contrast agent.

The procedure outlined in this paper involves several innovative refinements to standard micro-CT specimen preparation and analysis. First, to permit reproducible measurement of CBV, radio-opaque vascular casts were prepared under controlled pressure. Second, to permit regional comparisons, micro-CT images were registered to an MRI anatomical brain atlas. Third, to better reflect the contribution of local microvessels to CBV, major vessels were excluded from the analysis.

We also address the hypotheses that differences in CBV exist over anatomical brain regions and that highly active primary sensory cortical areas have a particularly rich vascularization to meet their high metabolic demands (Harrison et al., 2002; Harrison, 2006). Specifically, we examine the possibility that primary sensory cortex has a relatively high CBV in the non-stimulated condition, reflecting more dense patterns of vascularization.

Materials and methods

The steps to measure CBV in regions of the mouse brain were: (1) the cerebral vasculature was filled with Microfil (Flow Tech, Inc., Carver, MA, USA), a radio-opaque silicone rubber containing particulate lead chromate and lead sulfate and known for minimal shrinkage (Cortell, 1969); (2) micro-CT images were acquired; (3) micro-CT images were re-scaled to CBV units; (4) CBV images were co-registered to an MRI anatomical brain atlas; (5) CBV was measured over brain regions; (6) small vessel CBV (sv-CBV) was calculated by major vessel masking; (7) regional CBV values were analyzed. Each step is detailed in the following sections.

Filling the cerebral vasculature with microfil

Nine female C57BL/6 mice (Charles River Laboratories, Wilmington, MA, USA), weighing 17–25 g, were anesthetized with an intraperitoneal injection (IP) of 100 μg ketamine per gram of body weight (Pfizer, Kirkland, QC, Canada), 20 μg of xylazine per gram of body weight (Bayer Inc., Toronto, Canada) and 3 μg of the vasodilator, acepromazine maleate (Arras et al., 2001), per gram of body weight (Vetoquinol, Lavaltrie, QC, Canada), then given an IP injection of heparin (200 U) (Organon Canada Ltd., Toronto, Canada). The inferior vena cava and descending aorta were ligated. A 24-gauge IV catheter (Becton Dickinson Infusion Therapy System Inc., UT, USA) was inserted into the left ventricle, sealed in place using the adhesive Loctite 404 (McMaster-Carr, GA, USA) and connected to a pressure-controlled pump (Model PS/200, Living Systems Instrumentation, VT, USA). All incidental cuts were sealed. A slit in the right atrium provided outflow.

To minimize variation in CBV due to vessel inflation, the pressure at which Microfil polymerizes should be uniform. Warm heparinized (5 U/mL) phosphate buffered saline (Wisent Inc., St-Bruno, QC, Canada) was perfused at 50 mm Hg for 5 min at a filling rate of 2 mL/min, followed by Microfil at room temperature at 150 mm Hg for 10 min at a filling rate of 0.25 mL/min. The filling rate was determined based on the rate of volume change in a graduated cylinder containing the infusate. The pump was stopped, the slit in the right atrium sealed and the pump restarted at 30 mm Hg, approximating normal capillary pressure (Burton, 1972; Li, 2004). At this uniform pressure, the Microfil polymerized over 90 min at room temperature. Microfil has previously been shown to remain intravascular (Rennie et al., 2007); we quantified the completeness of the perfusions in a section that follows.

Acquiring micro-CT images

In preparation for micro-CT scans, dissected skulls (devoid of external soft tissue and lower jaw) were fixed for 12 h at 4 ± 1 °C in 10% buffered formalin phosphate (Fisher Scientific Company, Ottawa, Canada). To avoid partial volume and beam hardening artifacts, the skulls were decalcified in 5% formic acid (Fisher Scientific Company, Ottawa, Canada) at 50 °C for 24 h and then mounted in 1% agar (Sigma-Aldrich Co., St. Louis, MO, USA). Each micro-CT image was acquired over 2 h in which 720 views were obtained through 360° rotation with a GE eXplore Locus SP Specimen Scanner using peak voltage 80 kVp, current 80 μA and field of view at object of 20.48 mm. The measured line spread function had full-width-at-half-maximum of 24 μm and the modulation transfer function at 10% was 34 line pairs/mm, based on previous work (Marxen et al., 2004). The micro-CT images were reconstructed with isotropic cubic voxels of size 20 μm.

Measuring completeness of the perfusion

A potential source of error is incomplete perfusion of the brain with Microfil, leading to underestimated CBV. Thus, the proportion of vessels filled with Microfil was measured. Specifically, five of the perfused specimens were paraffin embedded and sixteen 5 μm coronal sections were cut: four samples (spaced 10 μm apart) were cut at four locations (defined by frontal cortex, striatum, hippocampus and superior colliculus). To calculate the percentage of vessels filled with Microfil, we stained the sections with hematoxylin and under 20× magnification, scored vessels in randomly selected fields according to whether Microfil was seen in the lumen. The data were categorized by specimen (out of 5) and brain location (out of 4). To test whether the completeness of Microfil perfusion significantly differed between the locations examined, an ANOVA was performed on a linear mixed effect model of the data, with one fixed effect (location) and one random effect (specimen) using the statistical program R, available at http://www.r-project.org/.

Re-scaling the micro-CT images to CBV units

The CBV of each tissue voxel is the ratio of the concentration of Microfil in that tissue voxel to the concentration of Microfil in the vasculature. This was computed for each micro-CT image, by using simple volume averaging of the components of the voxel, which were assumed to be Microfil and tissue. The tissue's radio-opacity is similar to 1% agar and is much lower than that of Microfil.

To study the relative radio-opacities of the components of each voxel, an additional C57BL/6 mouse was perfused just with PBS, without Microfil, prior to scanning. This specimen was imaged in 1% agar together with an external slab of Microfil and the average radio-opacity in all components was compared. We also tested uniformity in the CT intensity through the depth of the image, by measuring the percentage variation in the line profile through the tissue.

Each micro-CT image was re-scaled into CBV units by the following equation:

$$I_{\mathrm{CBV}} = 100(I_{\mathrm{ORIGINAL}} - I_{\mathrm{AGAR}}) / (I_{\mathrm{MICROFIL}} - I_{\mathrm{AGAR}}),$$

where I_{ORIGINAL} denotes the original intensity of the tissue voxels, I_{AGAR} denotes the average intensity of voxels in the 1% agar and I_{MICROFIL} denotes the average intensity of voxels completely filled with Microfil. The background intensity, I_{AGAR}, was computed as the average intensity of approximately 10,000 voxels in the 1% agar. We applied a custom written program to automatically trace vessel centerlines and determine vessel diameters. This automated vessel tracking program traces the centerlines of tubular objects by maintaining equal distance from the lumen wall as determined by the image intensity gradient along rays perpendicular to the vessel centerline (Fridman et al., 2004). To normalize the intensity of each individual image, I_{MICROFIL} was computed as the average intensity of approximately 20,000 voxels at centerline positions of vessel segments with diameter between 0.1 and

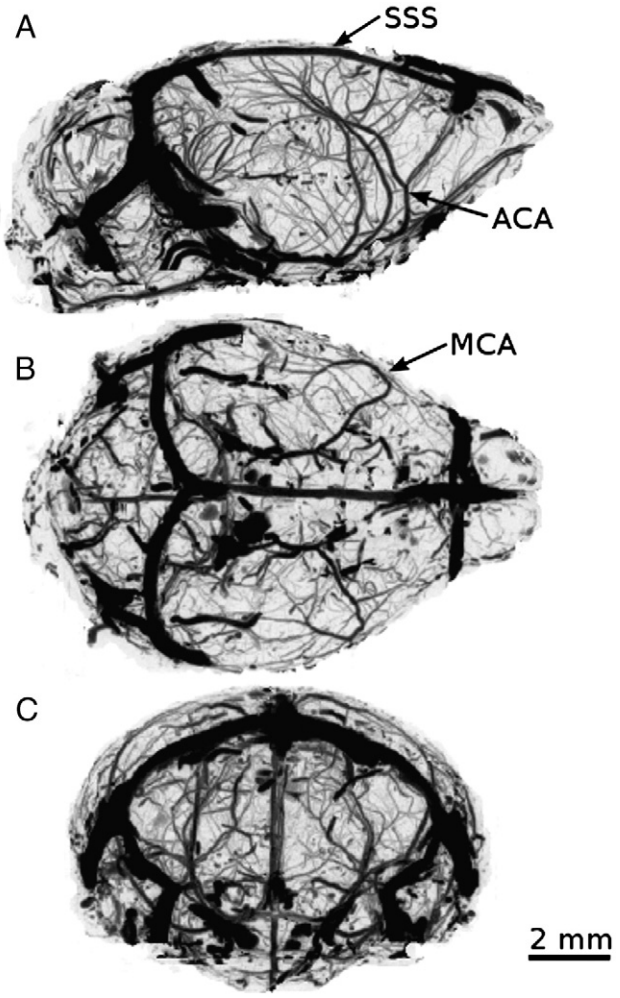

Fig. 1. Illustration of a representative maximum intensity projection of a micro-CT image in three views, (A) sagittal, (B) horizontal and (C) coronal. For illustrative purposes, the images have been cropped using an MRI derived mask to show only CT data within the brain. Marked with arrows are the middle cerebral artery (MCA), the anterior cerebral artery (ACA) and the superior sagittal sinus (SSS).

0.2 mm. Use of these vessel segments ensured that the voxels were completely filled with Microfil.

Co-registering micro-CT images to an MRI anatomical brain atlas

To delineate CBV measurement regions, we used an MRI anatomical brain atlas that was registered to the micro-CT images. The MRI anatomical brain atlas, which has 62 labeled 3D regions (Dorr et al., 2008), was prepared by averaging 20 female and 20 male C57BL/6 brain MRI images of 32 μm isotropic resolution (Spring et al., 2007). The MRI anatomical brain atlas was accessed at http://www.mouseimaging.ca/research/C57Bl6j_mouse_atlas.html.

Each micro-CT image was registered to the MRI anatomical brain atlas using vascular landmarks as a guide. As landmarks, we selected four easily identifiable bifurcations on major vessels in the mid-sagittal plane, which had low variability in position, namely: the branch point of the vertebral arteries and the basilar artery; the branch point of the medial orbitofrontal artery from the azygos of the anterior cerebral artery; the branch point of the rostral rhinal veins from the superior sagittal sinus; the branch point of the transverse sinuses from the superior sagittal sinus. The position of each landmark in the MRI anatomical brain atlas was computed as the mean value of the coordinates identified on a subset of eight of its individual MRI images. The computer program Register, which was used to identify landmarks is distributed by the Montreal Neurological Institute (http://www.bic.mni.mcgill.ca/software/). The same four landmarks were also identified on each of the micro-CT images by applying our automated vessel tracking program. The registration of micro-CT images to the MRI anatomical brain atlas was performed using a procrustes matching algorithm without scaling (Sibson, 1978) applied to each landmark position in the micro-CT images and the corresponding landmarks in the MRI anatomical brain atlas.

Measuring CBV over brain regions

Our goal was to reduce variability in CBV caused by registration error. Of the 62 regions in the MRI anatomical brain atlas, we selected all 13 regions that were larger than 5 mm^3. Selection of this threshold was based on a registration simulation that relied on the measured variability in the position of the vascular landmarks. This simulation involved generating five transformed copies of a given micro-CT image by adding random offsets derived from observed positional variation in vascular landmarks; for the transformed images the coefficient of variation (COV) was calculated region by region and an arbitrary cutoff at 10% COV led us to retain regions larger than 5 mm^3.

Misregistration error can significantly bias CBV when there is a great difference between the values of neighboring regions. To reduce

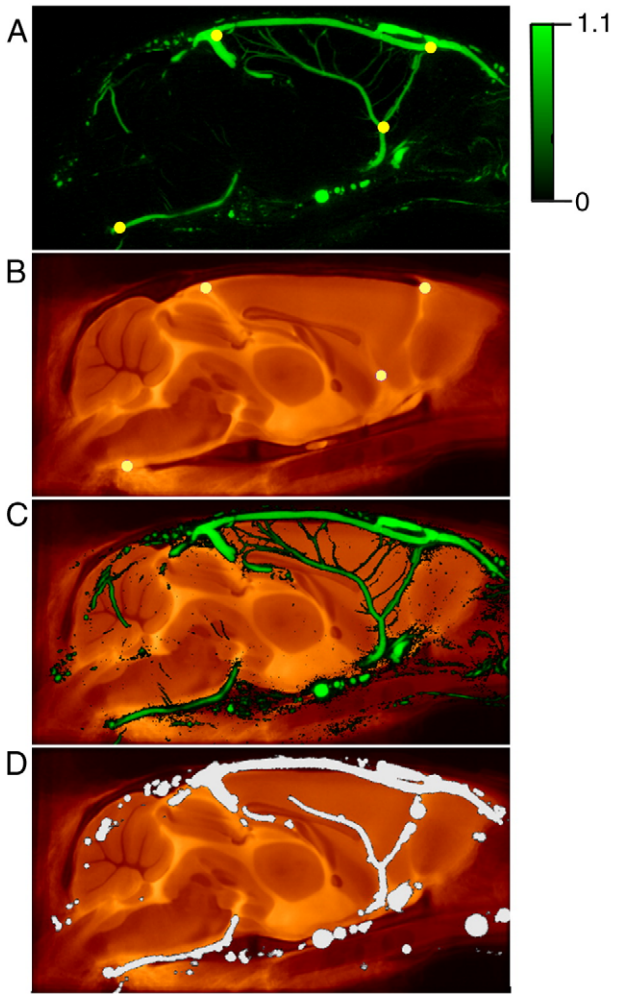

Fig. 2. The mid-sagittal section of a micro-CT image (A) and the corresponding section of the MRI anatomical brain atlas (B) with suitably chosen vascular landmarks (yellow) leads to accurate registration (C). Also shown is the corresponding major vessel mask (gray) superimposed on the MRI anatomical brain atlas (D).

this bias, we incrementally eroded the boundary of each region on the MRI anatomical brain atlas using a six neighbor binary morphological operator (Haralick et al., 1987). We selected 0.15 mm as the depth of erosion because the CBV values of gray matter regions that border white matter regions stabilized after this amount of erosion.

The following computational method was applied to obtain CBV values. The average CBV and standard error was calculated for each of the selected 13 brain regions. To map CBV over the cerebral cortex, we solved Laplace's equation to generate field-lines from the inner to the outer cortical surface. This method has previously been applied to map human cortical thickness (Jones et al., 2000) and has recently been adapted to determine cortical thickness in the mouse brain (Lerch et al., 2008). Next, CBV was averaged along each field-line and the value was projected to the mid-cortical surface; this was done through the entire thickness of the cortex, without eroding the boundary. To determine CBV through the depth of the cortex, the field-lines were divided into ten equal parts, which collectively defined ten layers.

Determining sv-CBV by major vessel masking

To emphasize the contribution of local microvessels to CBV, major vessels were excluded using a selectable diameter threshold that was arbitrarily chosen to be 100 μm. We formed a major vessel mask by our automated vessel tracking program to identify vessels in the micro-CT images greater than 100 μm in diameter. The metric, sv-CBV, was defined as the blood volume in a region from all voxels not covered by the major vessel mask as a percentage of the region's volume; sv-CBV was measured over the 13 brain regions and the cerebral cortex.

Analyzing regional CBV values

Using *R*, a statistical analysis was performed on the CBV data, which were categorized by specimen ($N = 9$), brain region ($N = 13$) and the type of metric (total CBV or sv-CBV). An ANOVA was performed on a linear mixed effect model of the data, which had two fixed effects (brain region and type of metric) and one random effect (specimen). The percentage difference between total CBV and sv-CBV was also determined for each micro-CT image.

To determine if sv-CBV significantly differed between brain hemispheres, ten of thirteen regions were segmented into portions in each hemisphere and the mean sv-CBV was graphically compared. An ANOVA was performed with R, using a mixed effect linear model where hemisphere was the fixed factor and specimen was the random factor.

To compare sv-CBV over regions of the cortex, the primary sensory areas were delineated on right and left cortical maps based on published maps for the C57BL/6 mouse, prepared by staining cytochrome oxidase (Airey et al., 2005), cytochrome oxidase and myelin (Hunt et al., 2006) and acetylcholinesterase (Paxinos and Franklin, 2003).

All described animal procedures were approved by the Hospital for Sick Children Animal Care Committee, subject to the Canadian Council on Animal Care.

Results

A representative example of one of the Micro-CT images is shown in three maximum intensity projection views in Fig. 1. All major arteries branching from the circle of Willis and major returning veins and sinuses were identifiable, such as the middle cerebral artery (MCA), the anterior cerebral artery (ACA) and the superior sagittal sinus (SSS) (marked with arrows in Fig. 1). Inspection of the images provided no evidence that Microfil had leaked outside of vessels.

Histological analysis revealed that over the group of mice the average ± standard error of mean (SEM) percentage of vessels filled with Microfil was 93 ± 3%, which may have been underestimated due to minor displacement of Microfil fragments during slide preparation.

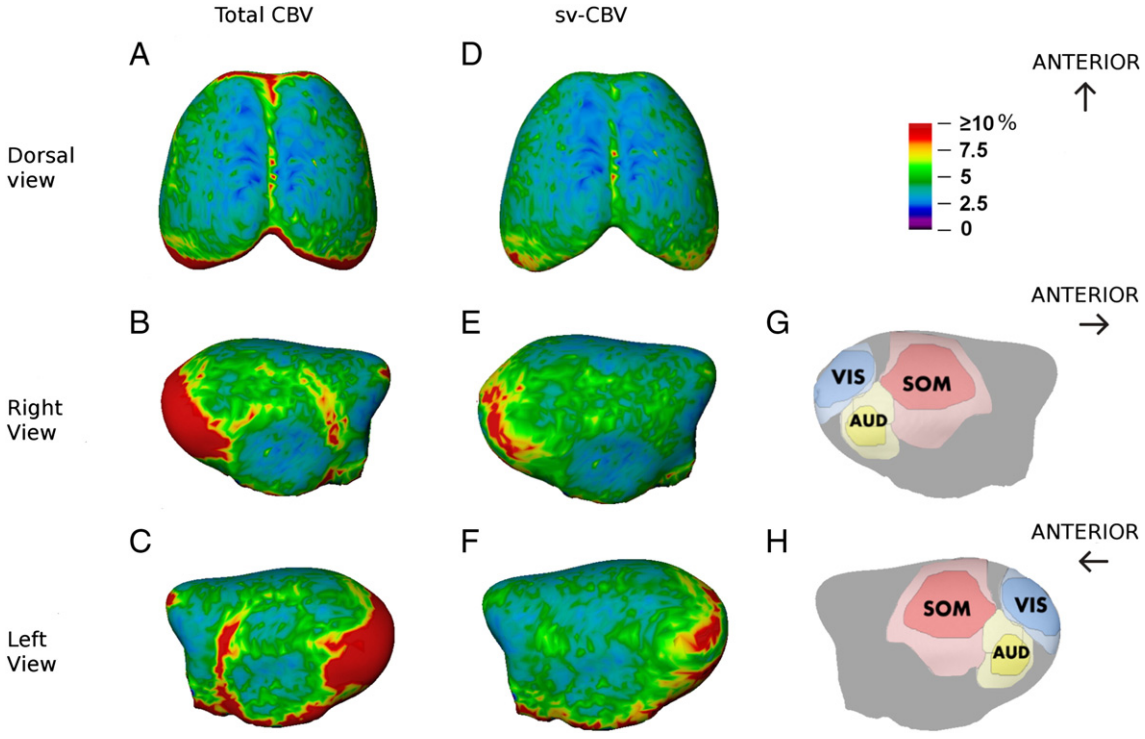

Fig. 3. CBV maps over the surface of the cerebral cortex, averaged over nine mice: (A-C) show total CBV maps for the dorsal, right lateral and left lateral surfaces, respectively; (D-F) show the sv-CBV maps; (G and H) show the right and left surfaces marked with manually delineated visual, auditory and somatosensory areas (in blue, yellow, and red respectively). For each sensory modality a core region (dark shading) is indicated, which includes visual areas V1 and V2 and auditory areas A1 and A2. The large somatosensory area (pink) denotes primary somatosensory areas including the extensive barrel cortex region.

Table 1
Total CBV and sv-CBV values for thirteen brain regions and the total brain reported as mean ± SEM.

Region	Total CBV (%)	sv-CBV (%)
Amygdala	4.3 ± 0.4	4.1 ± 0.4
Arbor vitae	4.0 ± 0.4	3.9 ± 0.3
Cerebral cortex	7.9 ± 0.7	4.6 ± 0.4
Cerebellar cortex	6.6 ± 0.5	4.9 ± 0.5
Corpus callosum	3.1 ± 0.5	2.9 ± 0.4
Hippocampus	3.7 ± 0.4	3.7 ± 0.4
Hypothalamus	4.3 ± 0.5	4.3 ± 0.5
Medulla	7.9 ± 0.5	5.7 ± 0.3
Midbrain	5.6 ± 0.6	4.7 ± 0.5
Olfactory bulbs	6.9 ± 0.4	5.9 ± 0.5
Pons	4.4 ± 0.5	4.3 ± 0.5
Striatum	2.8 ± 0.3	2.8 ± 0.3
Thalamus	3.7 ± 0.5	3.6 ± 0.5
Total brain	5.8 ± 0.4	4.4 ± 0.3

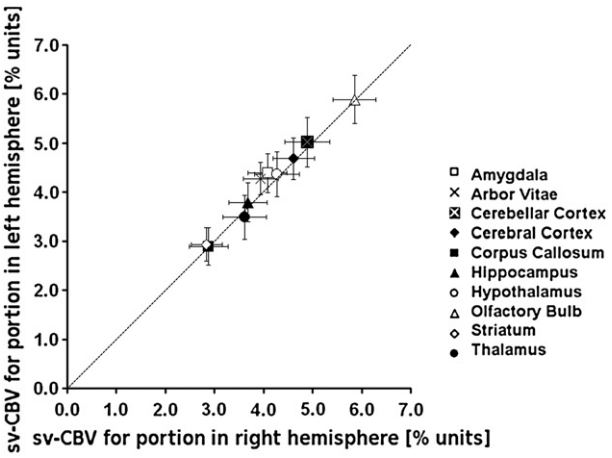

Fig. 5. Comparison of mean sv-CBV ± SEM for regions in left versus right hemisphere. For reference the line of identity has been plotted.

The completeness of Microfil perfusion did not significantly differ between the locations examined ($F = 0.72$, $p = 0.5$).

The average radio-opacities of Microfil and 1% agar were 3700 ± 100 Hounsfield units and 0 ± 100 Hounsfield units, respectively. In support of the assumption that CT intensity varies negligibly through the depth of images, we found that the line profile through the unperfused brain tissue had a maximum variation of 5 Hounsfield units.

A representative example of vascular-landmark registration of a micro-CT image to the anatomical brain atlas is shown in Fig. 2 (A,B,C). The mean value ($N = 9$) for the standard deviation of the registered coordinates of the four vascular landmarks was 0.15 mm.

A representative example of the overlay of a major vessel mask on the MRI anatomical brain atlas is shown in Fig. 2 (D). In regions where multiple vessels converged, the diameters of the vessels tended to be overestimated by our automated vessel tracking program.

Cortical maps of total CBV, averaged across nine mice, are shown in Fig. 3 (A,B,C) and maps of sv-CBV in Fig. 3 (D,E,F). The posterior cortex had an elevated sv-CBV compared to the average cortical sv-CBV of 4.6±0.4. The primary sensory areas that are delineated (Airey et al., 2005; Hunt et al., 2006; Paxinos and Franklin, 2003) in Fig. 3 (G,H) indicate a higher value of CBV in the primary visual and auditory areas relative to the average value of the cortex. However, there does not appear to be a higher than average value of the CBV in the primary somatosensory areas.

Table 1 summarizes CBV data sets for both total and sv-CBV. To illustrate the shapes, relative sizes and locations of the 13 brain regions, three sagittal slices have been labeled with each region in Fig. 4. Significant differences were found between regions ($F = 35.6$, $p < 0.0001$) and by type of metric, namely, total CBV or sv-CBV ($F = 28.8$, $p < 0.0001$). The largest differences between total CBV and sv-CBV were found in the cerebral cortex, the cerebellar cortex, the medulla oblongata, the olfactory bulbs and the midbrain, respectively. As shown in Fig. 5, sv-CBV did not significantly differ between hemispheres (F-value = 3.4, p-value = 0.07).

As plotted in Fig. 6, the variation in CBV through the depth of the cortex showed no fine structure but did show a monotonic increase from inside to outside for both sv-CBV and for total CBV. The curve for sv-CBV was flatter than the curve for total CBV. The difference

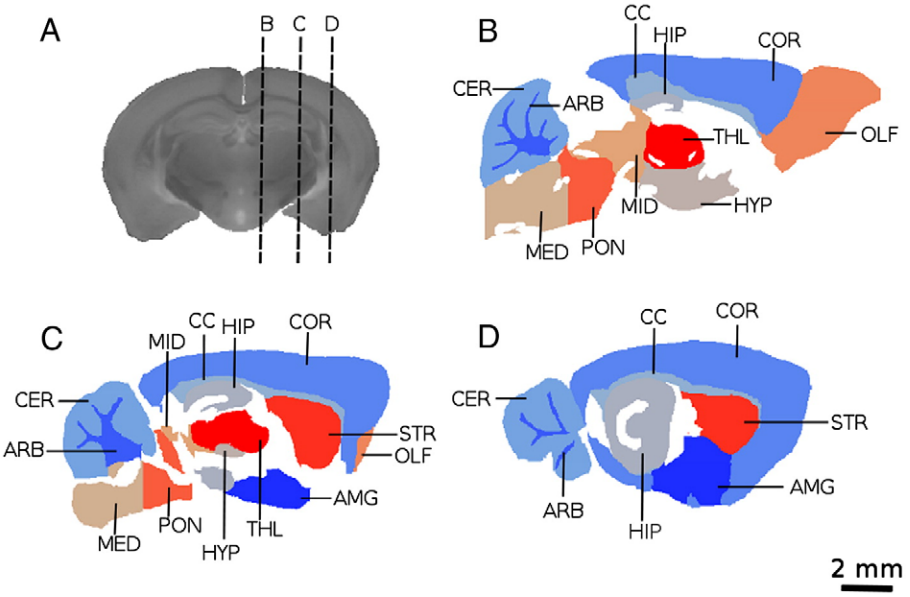

Fig. 4. Representation of 13 regions featured in Table 1 by labeling the area for each region in three sagittal slices (B-D). The relative positions of each sagittal slice are marked on a coronal image (A) from the 40 mouse average MRI image. AMG = amygdala, ARB = arbor vitae, COR = cerebral cortex, CER = cerebellar cortex, CC = corpus callosum, HIP = hippocampus, HYP = hypothalamus, MED = medulla oblongata, MID = midbrain, OLF = olfactory bulbs, PON = pons, STR = striatum, THL = thalamus.

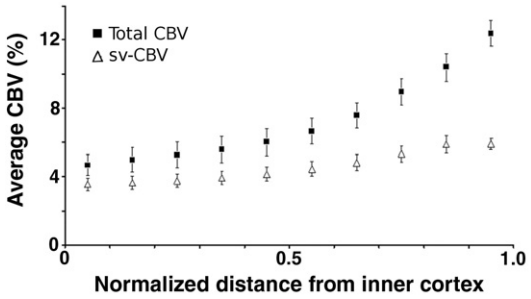

Fig. 6. Plot of mean CBV ± SEM versus the normalized distance from the inner surface of the cortex (value = 0) toward the outer surface (value = 1).

between the two curves was most pronounced at the outer surface of the cortex.

Discussion

This paper demonstrates the use of micro-CT to generate CBV maps of the mouse, an application that is of particular interest for characterizing cerebral vascular disease phenotypes. Several innovative refinements to standard micro-CT specimen preparation and analysis procedures were developed to meet this objective. To minimize variation due to vessel inflation, we perfused the vascular network at a specified pressure by controlling inflow and outflow of the contrast agent. To permit regional comparisons, micro-CT images were registered to an MRI anatomical brain atlas. By re-scaling the intensities to CBV units and masking out major vessels, the sv-CBV values better reflected the local contributions of microvessels; this protocol also permits flexible selection of major vessels masks. We provided normative values of CBV in thirteen brain regions, and cortical maps to illustrate normative variations in the brain.

The total brain CBV reported here can be compared with measurements obtained in vivo. A reported value of in vivo CBV measured using intravascular radionuclides is 35–40 μL of blood per gram of brain tissue (Edvinsson et al., 1973). By assuming a brain density of 1 g/mL, this method gives a total CBV of 3.5% to 4% in our scale. These values, which do not suppress the contributions of major vessels, are in reasonable agreement with our sv-CBV measurement of 4.4 ± 0.3%, but lower than the total CBV of 5.8 ± 0.4%. A possible explanation for this difference is that by preparing the radio-opaque vascular casts at a pressure of 30 mm Hg, the venous vessels, which contain most of the blood in the brain, were distended past their normal physiological point. Most of this effect would have been accounted for by masking of the major sinuses and veins. However, the remaining slight difference is likely owing to the large amount of blood in the venules, which may also be distended in the pressure control setup. Nevertheless, the CBV values measured in this paper are in reasonable agreement with the in vivo CBV values, as obtained using intravascular radionuclides.

To obtain reproducible values of CBV, we stress that the radio-opaque vascular casts must be prepared at a well-defined pressure. As the main contribution to the CBV comes from highly compliant venules and veins, failure to control this factor would likely lead to a large variation in results. We set the pressure close to an assumed average capillary pressure of about 30 mm Hg, which has not been directly measured in the mouse brain, but which provides a commonly accepted estimate for capillaries in the systemic circulation (Burton, 1972; Li, 2004). In this case, we can expect the sv-CBV values to be similar to the in vivo value. The close correspondence of sv-CBV between bilaterally symmetric regions (see Fig. 5) supports the notion that the image registration was accurate. Another factor affecting reproducibility is the completeness of major vessel masking. The purpose of applying our automated vessel tracking program was to ensure greater accuracy of the major vessel masking. Since vessels with diameter greater than 100 μm represent approximately 1% of total brain volume, moderate overestimate of the mask can be expected to have a negligible effect on sv-CBV. Masking of finer vessels in the brain could also be performed, in future, with micro-CT scanners of higher resolution and signal-to-noise ratio.

As brain atlases become more refined, one likely interest will be to measure sv-CBV in increasingly fine regions. In such cases, registration will pose a fundamental limitation on the size of the region over which sv-CBV can be accurately mapped. The registration method used in this paper was based on vascular landmarks that have 0.15 mm root mean squared variability in position. In Fig. 3, a comparison is made between total CBV and sv-CBV. By masking the major vessels, the sv-CBV was shown to be more spatially uniform over structurally similar regions of the cortex. The ability to mask vessels also poses a limitation on the size of the region that can be studied. In small regions, a major vessel may constitute a large fraction of the measurement volume; this artifact could outweigh microvascular variation and lead to false interpretation. For example, a 100 μm vessel that passes through a measurement volume of 1 mm^3 will increase an average CBV of 4% to about 5%, leading to a 25% overestimate. Since the masking is a function of resolution and SNR, improvements in micro-CT image quality will translate to greater control of the size of the region that can be mapped.

One of our scientific questions was whether primary sensory areas of cortex have a higher local sv-CBV compared to other cortical regions. This question was based on the hypothesis that sensory input areas such as visual, auditory and somatosensory cortices are highly active, with metabolic demands that might be met with a privileged blood oxygen supply. It is well known from hemodynamic based functional imaging techniques such as optical imaging of intrinsic signals (Grinvald et al., 1986) that under sensory stimulation, there is a significant CBV change in primary cortex compared to less active association cortex (Harrison et al., 1998; Harel et al., 2000). Although the changes described in these studies are transient responses to stimulation, it is possible that primary sensory cortex has a more permanent vascular specialization (Harrison et al., 2002). Comparison of the cortical map of sv-CBV in Fig. 3 with maps showing locations of the major sensory cortical areas, suggests that sv-CBV is elevated in both visual and auditory areas, though not convincingly in the primary somatosensory area. This likely suggests that there is not a specialized blood supply for the entire somatosensory area. One reason for this may be that the hypothesized increased blood oxygen supply to highly active brain areas may be most readily detectable at the capillary network level (Harrison et al. 2002) whereas this definition of sv-CBV includes feeding arterioles and drainage venules that contain a significant proportion of the blood.

The sv-CBV increased from the inner to the outer boundary of the cerebral cortex, which was consistent with the depth variation of cortical microvessel density observed with confocal microscopy in rats for vessels with diameter under 50 μm (Masamoto et al., 2004) and in humans both with and without major vessel masking above 10 μm in diameter (Lauwers et al., 2008). Unlike those studies of microvessel density, however, the sv-CBV, plotted in Fig. 6, did not sharply decline at the outer boundary, but appeared to level off toward the outer 20% of the depth. This pattern of variation supports a model of vascular organization where capillary-rich beds and their associated feeding arterioles and drainage venules are concentrated near the outer boundary of the cortex.

Mapping sv-CBV over an anatomical brain atlas could lead to better understanding of vascular degeneration in dementia models, as well as the angiogenesis following treatments. Our method of sv-CBV mapping improves on past work as it can be used to determine CBV phenotypes in small 3D regions of the mouse brain. With continued development of better mouse brain atlases and genetic models, we anticipate that this method to measure sv-CBV will lead to a better characterization of vascularity in mouse models of cerebral vascular disease.

Disclosure/conflict of interest

We have no conflict of interest.

Acknowledgments

We would like to thank Marvin Estrada of the Lab Animal Services at the Hospital for Sick Children for valuable advice in developing the surgical procedure. We would also like to thank Professor Bojana Stefanovic of the Sunnybrook Health Sciences Centre for her helpful suggestions.

Funding for this research was provided by the Canadian Institutes of Health Research with Funding Reference Number 86734.

References

Airey, D.C., Robbins, A.I., Enzinger, K.M., Wu, F.B., Collins, C.E., 2005. Variation in the cortical area map of C57BL/6J and DBA/2J inbred mice predicts strain identity. BMC Neurosci. 6 (18), 1–8.

Arras, M., Autenried, P., Rettich, A., Spaeni, D., Rulicke, T., 2001. Optimization of intraperitoneal injection anesthesia in mice: drugs, dosages, adverse effects, and anesthesia depth. Comp. Med. 51, 443–456.

Buee, L., Hof, P.R., Delacourte, A., 1997. Brain microvascular changes in Alzheimer's disease and other dementias. Ann. N.Y. Acad. Sci. 826, 7–24.

Burton, A.C., 1972. Physiology and Biophysics of the Circulation, 2nd edn. Year Book Medical Publishers, Chicago, IL.

Cortell, S., 1969. Silicone rubber for renal tubular injection. J. Appl. Physiol. 26, 158–159.

Dorr, A., Sled, J.G., Kabani, N., 2007. Three-dimensional cerebral vasculature of the CBA mouse brain: a magnetic resonance imaging and micro computed tomography study. NeuroImage 35, 1409–1423.

Dorr, A.E., Lerch, J.P., Spring, S., Kabani, N., Henkelman, R.M., 2008. High resolution three-dimensional brain atlas using an average magnetic resonance image of 40 adult C57Bl/6J mice. NeuroImage 42, 60–69.

Edvinsson, L., Nielsen, K.C., Owman, C.H., 1973. Circadian rhythm in cerebral blood volume of mouse. Specialia 29, 432–433.

Fridman, Y., Pizer, S.M., Aylward, S., Bullitt, E., 2004. Extracting branching tubular object geometry via cores. Med. Image Anal. 8, 169–176.

Goodenough, D.J., Weaver, K.E., Costaridou, H., Eerdmans, H., Huysmans, P., 1986. A new software correction approach to volume averaging artifacts in CT. Comput. Radiol. 10, 87–98.

Grinvald, A., Lieke, E., Frostig, R.D., Gilbert, C.D., Wiesel, T.N., 1986. Functional architecture of cortex revealed by optical imaging of intrinsic signals. Nature 324, 361–364.

Haralick, R.M., Sternberg, S.R., Zhuang, X.H., 1987. Image-analysis using mathematical morphology. IEEE Trans. Pattern Anal. Mach. Intelligence 9, 532–550.

Heinzer, S., Krucker, T., Stampanoni, M., Abela, R., Meyer, E.P., Schuler, A., Schneider, P., Muller, R., 2006. Hierarchical microimaging for multiscale analysis of large vascular networks. NeuroImage 32, 626–636.

Harrison, R.V., Harel, N., Kakigi, A., Raveh, E., Mount, R.J., 1998. Optical imaging of intrinsic signals in chinchilla auditory cortex. Audiology & Neurotology 3, 214–223.

Harrison, R.V., 2006. Development, maintenance and plasticity of tonotopic projections from cochlea to auditory cortex, In: Lomber, S, Eggermont, J (Eds.), Reprogramming the Cerebral Cortex: Plasticity Following Central and Peripheral Lesions, 1st edn. Oxford, New York, NY, pp. 159–180.

Harrison, R.V., Harel, N., Panesar, J., Mount, R.J., 2002. Blood capillary distribution correlates with hemodynamic-based functional imaging in cerebral cortex. Cereb. Cortex 12, 225–233.

Harel, N., Mori, N., Sawada, S., Mount, R.J., Harrison, R.V., 2000. Three distinct auditory areas of cortex (AI, AII, and AAF) defined by optical imaging of intrinsic signals. NeuroImage 11, 302–312.

Hunt, D.L., Yamoah, E.N., Krubitzer, L., 2006. Multisensory plasticity in congenitally deaf mice: how are cortical areas functionally specified? Neuroscience 139, 1507–1524.

Jones, S.E., Buchbinder, B.R., Aharon, I., 2000. Three-dimensional mapping of cortical thickness using laplace's equation. Hum. Brain Mapp. 11, 12–32.

Langheinrich, A.C., Michniewicz, A., Bohle, R.M., Ritman, E.L., 2007. Vasa vasorum neovascularization and lesion distribution among different vascular beds in ApoE (−/−)/LDL−/− double knockout mice. Atherosclerosis 191, 73–81.

Li, J.K., 2004. Dynamics of the Vascular System, 1st edn. World Scientific Publishing Company, Singapore.

Lerch, J.P., Carroll, J.B., Dorr, A., Spring, S., Evans, A.C., Hayden, M.R., Sled, J.G., Henkelman, R.M., 2008. Cortical thickness measured from MRI in the YAC128 mouse model of Huntington's disease. NeuroImage 46, 243–251.

Lauwers, F., Cassot, F., Lauviers-Cances, V., Puwanarajah, P., Duvernoy, H., 2008. Morphometry of the human cerebral cortex microcirculation: general characteristics and space-related profiles. NeuroImage 39, 936–948.

Marxen, M., Thornton, M.M., Chiarot, C.B., Klement, G., Koprivnikar, J., Sled, J.G., Henkelman, R.M., 2004. MicroCT scanner performance and considerations for vascular specimen imaging. Med. Phys. 31, 305–313.

Masamoto, K., Kurachi, T., Takizawa, N., Kobayashi, H., Tanishita, K., 2004. Successive depth variations in microvascular distribution of rat somatosensory cortex. Brain Res. 995, 66–75.

Paxinos, G., Franklin, K.B.J., 2003. The Mouse Brain in Stereotaxic Coordinates: Compact, Second Ed. Academic Press.

Rennie, M.Y., Whiteley, K.J., Kulandavelu, S., Adamson, S.L., Sled, J.G., 2007. 3D visualisation and quantification by microcomputed tomography of late gestational changes in the arterial and venous feto-placental vasculature of the mouse. Placenta 28, 833–840.

Ritman, E.L., 2004. Micro-computed tomography-current status and developments. Annu. Rev. Biomed. Eng. 6, 185–208.

Sibson, R., 1978. Studies in the robustness of multidimensional scaling: procrustes statistics. J. R. Stat. Soc., Ser. B 40, 234–238.

Spring, S., Lerch, J.P., Henkelman, R.M., 2007. Sexual dimorphism revealed in the structure of the mouse brain using three-dimensional magnetic resonance imaging. NeuroImage 35, 1424–1433.

Toga, A.W., Mazziotta, J.C., 2002. Brain Mapping: The Methods, 2nd edn. Academic Press, San Diego, CA.

Verant, P., Serduc, R., Van der Sanden, B., Remy, C., Vial, J.C., 2007. A direct method for measuring mouse capillary cortical blood volume using multiphoton laser scanning microscopy. J. Cereb. Blood Flow Metab. 27, 1072–1081.

Wu, E.X., Wong, K.K., Andrassy, M., Tang, H.Y., 2003. High-resolution in vivo CBV mapping with MRI in wild-type mice. MRM 49, 765–770.